ACS OMEGA

http://pubs.acs.org/journal/acsodf

Article

Valorization of Ginger Waste-Derived Biochar for Simultaneous Multiclass Antibiotics Remediation in Aqueous Medium

Roshni Meghani, Vaibhavi Lahane, Sumana Y. Kotian, Sneh Lata, Swati Tripathi, Kausar M. Ansari, and Akhilesh K. Yadav*

Cite This: *ACS Omega* 2023, 8, 11065−11075

Read Online

ACCESS | Metrics & More | Article Recommendations | Supporting Information

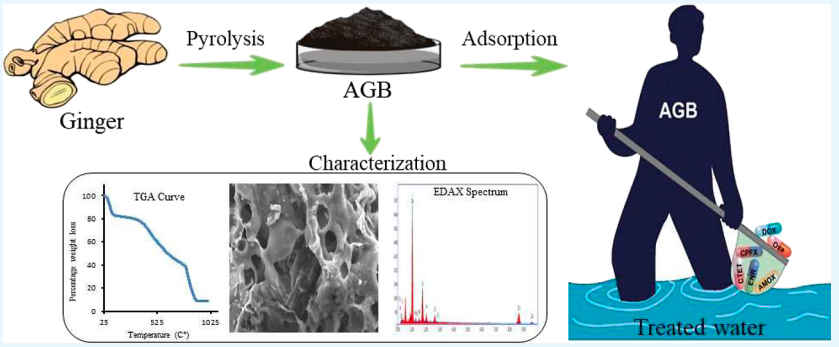

ABSTRACT: The presence of antibiotics in the aqueous environment has been a serious concern primarily due to the development of antimicrobial resistance (AMR) in diverse microbial populations. To overcome the rising AMR concerns, antibiotic decontamination of the environmental matrices may play a vital role. The present study investigates the use of zinc-activated ginger-waste derived biochar for the removal of six antibiotics belonging to three different classes, viz., β-lactams, fluoroquinolones, and tetracyclines from the water matrix. The adsorption capacities of activated ginger biochar (AGB) for the concurrent removal of the tested antibiotics were investigated at different contact times, temperatures, pH values, and initial concentrations of the adsorbate and adsorbent doses. AGB demonstrated high adsorption capacities of 5.00, 17.42, 9.66, 9.24, 7.15, and 5.40 mg/g for amoxicillin, oxacillin, ciprofloxacin, enrofloxacin, chlortetracycline, and doxycycline, respectively. Further, among the employed isotherm models, the Langmuir model fitted well for all the antibiotics except oxacillin. The kinetic data of the adsorption experiments followed the pseudo-second order kinetics suggesting chemisorption as the preferred adsorption mechanism. Adsorption studies at different temperatures were conducted to obtain the thermodynamic characteristics suggesting a spontaneous exothermic adsorption phenomenon. AGB being a waste-derived cost-effective material shows promising antibiotic decontamination from the water environment.

1. INTRODUCTION

Since the discovery of penicillin in 1928, many molecules have made their way into the field of medicine and have proved to be a blessing in disguise to mankind. In fact, antibiotics have been a life-saving discovery since various classes of antibiotics have emerged and are being used for the treatment of mild to severe diseases. With the escalated usage of antibiotics for human and veterinary healthcare, these drugs has led to the emerging concern of antibiotic contamination in various environmental niches. Environmental antibiotic contaminations may be a leading cause of global threat of antibiotic resistance. The World Health Organization has termed antibiotic resistance a possible calamity of the 21st century.[1] As cited in the reports of the Centers for Disease Control and Prevention, approximately two million people in the United States get infected by the microbes that have become resistant to one or more antibiotic drugs and around twenty-three thousand deaths are caused each year due to the inability of the drug to treat the infection anymore.[2] Studies suggest that the unceasing increase in the resistance could bring about the deaths of approximately 10 million people and a Gross Domestic Product (GDP) reduction of 2−3.5 per cent, by 2050.[3] Untreated effluents from drug manufacturing industries and hospital sewage introduce antibiotic residues into the water bodies directly.[4,5] At the same time, the unregulated use of veterinary antibiotics in poultry and livestock is another significant source of contamination of these residues in water bodies and food items, such as meat and milk.[6−8] Antibiotics, as

Received: December 12, 2022
Accepted: February 22, 2023
Published: March 20, 2023

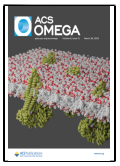

ACS Publications

© 2023 The Authors. Published by American Chemical Society

contaminants, have been reported in several environmental niches where water bodies being the primary reservoir potentially transmit these drugs to the food chains.[9,10] The microbes present in the water bodies evolve over time and develop immunity due to the prolonged presence of antibiotics.[11]

Remediation of antibiotic residues from different environments has been a global focus of research in recent decades. Various adsorbents have been developed for cost-effective adsorptive removal of these contaminants with varying adsorption capabilities.[12−14] Waste biomass-derived biochar-based adsorbents, being an economical and green approach, has gained significant attention for removal of various contaminants including antibiotics from various environmental niches.[15−18] Besides the source, the properties and remediation efficiency of biochar are dependent on temperature, particle size, heating rate, and pressure.[19−21] Additionally, the pore size, diameter, and surface area of the developed biochar play an important role in their adsorption capabilities. The efficiency and performance can be enhanced using various methods such as thermal air activation, ash pretreatment, alkali or acid pretreatment, or activation with a metal. Several studies have been performed for the removal of antibiotics from the aqueous environment, for example, Alnajrani and Alsager[22] demonstrated the use of a polymer of intrinsic microporosity for the removal of four commonly used antibiotics from the water matrix, while another study using the functionalized biochar presented the competitive adsorption of sulfonamides and chloramphenicol.[15] Furhter, Mei et al.[23] demonstrated the use of rice straw biochar-mediated removal of tetracycline. The study highlighted manifold increase in maximum adsorption capacity, reaching up to 156 mg/g, of biochar upon activation with urea and $FeCl_3$. Most of the available reports on the environmental antibiotic remediation lack a comprehensive solution targeting the concurrent removal of antibiotic drugs belonging to different structurally diverse chemical classes using an economically viable adsorbent.

The present study targets the simultaneous removal of the six widely used antibiotics belonging to different classes such as tetracyclines (doxycycline and chlortetracycline), β-lactams (amoxicillin and oxacillin), and quinolones (ciprofloxacin and enrofloxacin) using the zinc-activated ginger-waste biochar. To the best of our knowledge, this is the first application of ginger-waste-derived biochar for the removal of multiclass antibiotics from the aqueous environment. In this study, ginger waste was pyrolyzed to prepare the biochar which was further activated with zinc chloride to increase the adsorbent surface area and porosity resulting in enhanced adsorption capacity. The prepared cost-effective and eco-friendly activated ginger biochar (AGB) was evaluated for its removal efficiencies toward tested antibiotics using different parameters, viz., varying contact times, temperatures, pH, and adsorbate and adsorbent doses. The adsorption mechanism was also studied by conducting the kinetic (pseudo-first order, pseudo-second order, Elovich, and IPD models), isothermal (Langmuir, Freundlich, Temkin, Sips, and Dubinin−Radushkevich models), and thermodynamic studies.

2. MATERIALS AND METHODS

2.1. Raw Material and Chemicals. Ginger purchased from the local market was used for the preparation of the biochar which was activated with zinc using an electric muffle furnace (Thermo Scientific, USA). The adsorption experiments were performed in Milli-Q water on an orbital rotary shaker. Antibiotic analytical standards (amoxicillin, oxacillin, ciprofloxacin, enrofloxacin, doxycycline, and chlortetracycline) were purchased from Sigma-Aldrich (Missouri, USA). The adsorptive removal efficiencies were monitored using the Sciex Triple TOF5600+ (AB Sciex, Massachusetts, USA) equipped with an ultra-pressure liquid chromatography (Exion) system consisting the binary pumps, autosampler, column oven, and PDA detector.

2.2. Preparation of AGB. For the AGB preparation, the ginger was washed, cleaned, and boiled for 1 h. The mushy residue was separated by a sieve and air-dried. The dried ginger was then macerated into a fine powder and subjected to pyrolysis at 450 °C to obtain the biochar. For activation of the biochar, the prepared biochar was weighed and mixed with zinc chloride (1:2; w/w) with a few drops of Milli-Q to form a paste. The paste was kept at 40 °C overnight and was further subjected to pyrolysis in the electric furnace at 450 °C. The prepared zinc-activated biochar was washed with Mili-Q multiple times, dried, and used for experiments.

2.3. Characterization of AGB. The surface area, pore volume, and diameter were estimated by the Brunauer−Emmett−Teller (BET) instrument (Quanta chrome Instruments, USA). Thermal stability was analyzed by a thermogravimetric analyzer (TGA) [Mettler Toledo Stare, Columbus]. The functional group analysis of the prepared biochar was determined using attenuated total reflectance-Fourier transform infrared (ATR-FTIR), [Thermo Fisher (Nicolet iS5)] in the range of 400−4000 cm^{-1}. Morphological characterization of the prepared biochar was done using scanning electron microscopy (SEM) [QUANTA-250, FEI (Netherlands)].

2.4. Batch Adsorption Experiments. Batch adsorption experiments were conducted to check the adsorption patterns of amoxicillin, oxacillin, ciprofloxacin, enrofloxacin, doxycycline, and chlortetracycline onto the AGB. The AGB (1000 mg/L) was added to the flasks containing 20 mL water with an analyte concentration of 2 ppm for each antibiotic. The experiments were conducted with varying parameters of contact time, temperature, adsorbent and analyte dose, and pH. The generated data under different experimental conditions were subjected to kinetics, isothermal, and thermodynamic studies.

2.5. Analytical Quantification of the Adsorption Efficiencies. The qualitative and quantitative monitoring of the adsorption behaviour of tested antibiotics on the AGB was done using the Sciex QTof 5600+ equipped with an Exion LC system. The chromatographic separation was achieved using the stationary phase Kinetics C18 column (100 × 2.1 mm, 1.7 μm) using a gradient elution of mobile phase A (Water containing 1% formic acid) and B (ACN) as follows: 0−2 min 5% B; 2−9 min 5−60% B; 9−11 min 90% B; 11−12 min 90% B. The column was equilibrated with the initial mobile phase concentration between the consecutive injections. MS source parameters were set as follows: nebulizer (GS1), drying (GS2), and curtain (CUR) gases at 50, 50, and 32 psi, respectively; desolvation temperature at 550 °C; ion spray voltage at 5500 (ESI+). The compound-specific parameters, that is, declustering potential (DP) and collision energy (CE) were kept at 100 V and 5 V, respectively. ESI-MS molecular ion peaks ($[M + H]^+$) of amoxicillin (m/z 366.1039), oxacillin (m/z 332.1335), ciprofloxacin (m/z 402.1031), enrofloxacin (m/z 360.1642), chlortetracycline (m/z 479.1108), and doxycycline (m/z 445.1503) were used for quantification.The generated data were analyzed using Analyst ver. 1.8 and MultiQuant ver. 2.0

https://doi.org/10.1021/acsomega.2c07905
ACS Omega 2023, 8, 11065−11075

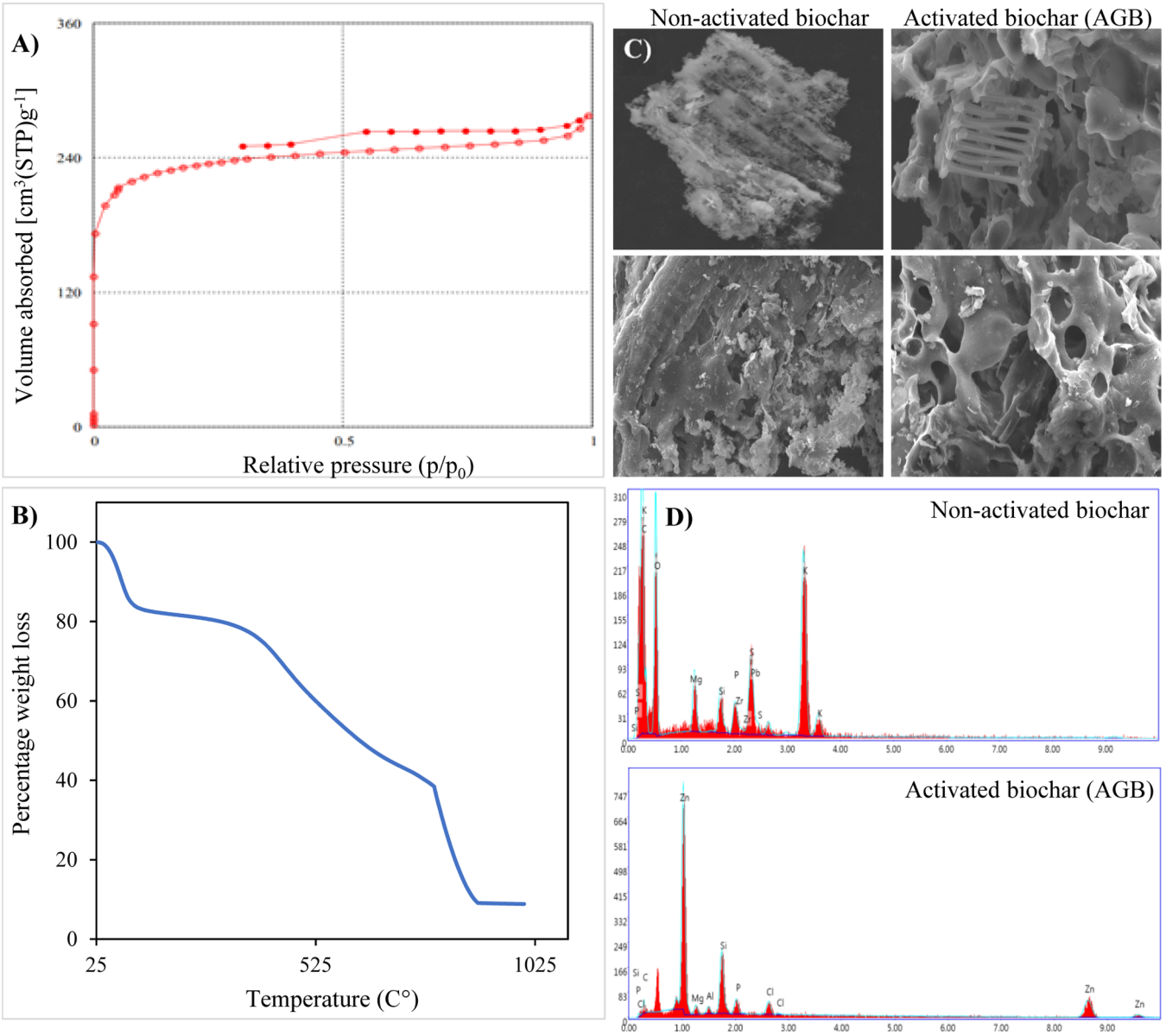

Figure 1. Adsorption−desorption isotherm (A) and TGA curve (B) of the AGB; scanning electron microscope images (C) and EDAX spectra (D) for non-activated and activated biochar.

software. The method was optimized and validated for its limits of detection and quantitation. Calibration curves for the tested antibiotics were performed with five different concentration range (3.9−125 ppb) by plotting the peak area versus concentrations. Good linearity (R^2 > 0.99) was achieved in the investigated range for tested analytes. The experimentally calculated limit of detections (LODs) and limit of quantifications (LOQs) obtained were 1.09, 3.61 ppb (amoxicillin); 0.25, 0.84 ppb (oxacillin); 0.30, 0.99 ppb (ciprofloxacin); 0.49, 1.63 ppb (enrofloxacin); 1.14, 3.78 ppb (chlortetracycline), and 0.93, 3.06 ppb (doxycycline), respectively. Representative extracted ion chromatograms (XICs) and mass spectra of the antibiotics are given as Supporting Information (Figures S1 and S2).

2.6. Statistical Analysis. Linear calibration curves for calculating the mass spectrometric limits of detection and quantification of antibiotics were calculated using Prism 5.0 software package (Graph Pad, USA), and data were reported as mean values obtained from three independent experiments. Statistical estimates (standard deviations, goodness of fit) between the control and biochar treatments were performed using Microsoft Excel for Windows 10 Pro.

3. RESULTS AND DISCUSSION

Preliminary experiments were performed with the native non-activated ginger biochar to study its adsorption efficiency toward the target antibiotics along with the zinc chloride-activated biochar. The non-activated biochar was less efficient in the removal of antibiotics in comparison to AGB (results not mentioned). $ZnCl_2$ being a Lewis acid is used as a dehydration agent for specific removal of the H and O from biomass to prevent the tar formation resulting in increased high surface area, active sites, and biomass porosity.[24,25] In recent times, it has been used as an efficient chemical activation agent for the fabrication of the porous carbonaceous material from a varied range of biomasses.[26] The differential adsorption behaviors of

https://doi.org/10.1021/acsomega.2c07905
ACS Omega 2023, 8, 11065−11075

non-activated and activated biochar were in agreement with the obtained BET and SEM data.

3.1. Characterization. The biochar was characterized using BET, SEM-EDAX, TGA, and FTIR analysis. The BET analyzer calculated the surface area, mean pore diameter, and total pore volume to be 577.2 m^2/g, 2.96 nm, and 0.428 cm^3/g, respectively, for the AGB, while for the non-activated biochar surface area, mean pore diameter and total pore volume were 1.188 m^2/g, 178.15 nm, and 0.052 cm^3/g, respectively. The increased surface area and porosity of the AGB supported enhanced adsorption capacity of the AGB compared to the native biochar. The hysteresis loop from the BET plot for the adsorption and desorption of N_2 in activated ginger biochar corresponding with H4 type (in reference to IUPAC classification) suggested the presence of micro as well as mesopores promoting a favorable and efficient adsorptive removal (Figure 1A).[26] Thermogravimetric curve for the activated biochar showed a weight loss of approximately 20 per cent up to 115 °C, while the weight remained nearly constant up to 400 °C. Again, the loss in weight was observed from 400 to 900 °C and attaining equilibrium thereafter. Thus, the TGA analysis depicted the significant stability of the adsorbent till 400 °C (Figure 1B).

The surface morphology presented by SEM analysis suggested a rough and porous surface of AGB (Figure 1C). The magnified image illustrated narrow slit-shaped pores, also evident from the H4 type BET adsorption−desorption plot. The SEM image for the non-activated biochar showed a rough non-porous surface. SEM-EDAX analysis performed on the AGB demonstrated the distribution of metals on its surface. Further, the point analysis done at various points showed the average percentage of zinc to be 32.44 followed by carbon at 31.96 per cent and oxygen at 20.89 per cent along with the presence of trace amounts of Si, Mg, and Al (Figure 1D).

The functional group study of the AGB showed a weak broad band at 3191 cm^{-1} suggesting the presence of the −OH group. The band at 1573 and 1637 cm^{-1} represent medium stretching vibrations from C═C and bending vibrations from N−H, respectively. A strong band at 1095 and 1000 cm^{-1} corresponds to the C−O stretching from secondary alcohol (Figure 2). The abundance of the electropositive metals (as evident by EDAX analysis) and the π-bonds (C═C) in AGB may facilitate the interaction between the adsorbent and adsorbate molecules via electrostatic and $\pi-\pi$ interactions enabling efficient chemisorption of the target contaminants on the AGB surface.[27−29] The chemisorption as an adsorption phenomenon for removal of antibiotics from water has also been supported by the kinetic data which supports the hypothesis of chemical interaction-mediated adsorption of target contaminants.

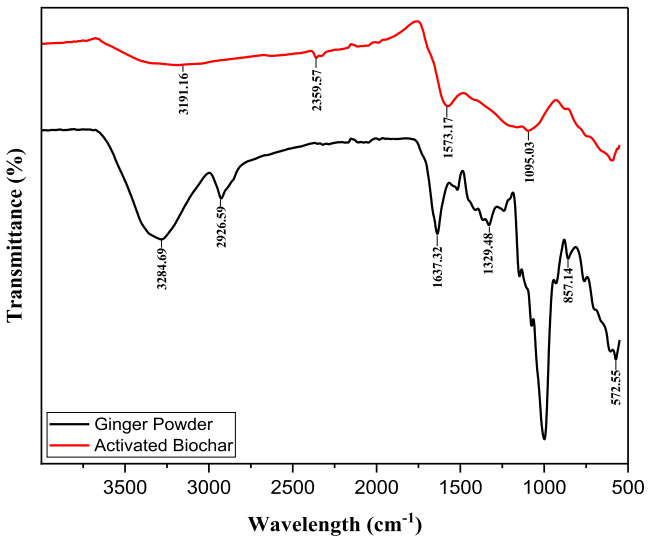

Figure 2. FTIR spectra of activated biochar (AGB) and ginger powder.

3.2. Factors Affecting Adsorption. The experiment to study the effect of contact time was conducted at 30 °C for 10−300 min in a 2 ppm spiked solution of 20 mL water with 20 mg of ginger biochar. The adsorption of antibiotics increased with the increasing contact time due to the readiness of adsorption sites for interactions with the adsorbate molecules attaining the maximum adsorption at 240 min. Oxacillin, ciprofloxacin, and enrofloxacin showed the strongest competitive interaction with AGB in the order oxacillin > ciprofloxacin ≥ enrofloxacin attaining the 84, 57, and 60 per cent adsorption, respectively, at 5 min. The adsorption affinity of amoxicillin was the weakest, among the tested antibiotics, exhibiting approximately 20 per cent adsorption at 3 h attaining a sharp increase between 3 and 4 h. A strong desorption phenomenon with approximately 32 per cent desorption from 4 to 5 h was observed reconfirming the weak interaction of amoxicillin on the adsorbent surface, while oxacillin, ciprofloxacin, and enrofloxacin showed either no or minimal desorption behavior confirming a strong and stable interaction with the AGB up to 5 h (Figure 3A). The pH levels of the aqueous medium play a decisive role in governing the interaction of the adsorbate and adsorbent. The optimization of the effect of pH on the adsorption efficiency was evaluated in the pH range of 2−10. The highest adsorption of antibiotics on AGB was observed at pH 6. Oxacillin showed a similar adsorption behavior also at pH 2. Fluoroquinolones (ciprofloxacin and enrofloxacin) showed a stable adsorption behavior across the varied pH ranges (Figure 3B). To check the effect of the adsorbent doses, the concentration of antibiotics was varied from 2 to 10 ppm in 1 mg/mL preparation of biochar in water. The maximum adsorption efficiency was shown at a concentration of 2 ppm for all the tested antibiotics. The increase in the number of adsorbent molecules has a negative impact on the competitive interaction of the individual antibiotics with the adsorbate surface probably due to the limited interaction sites on the AGB surface. Oxacillin showed a quite stable and strong adsorption behavior irrespective of the adsorbent concentration supported by the evidence obtained in the contact time and varied pH experiments (Figure 3C). The effect of the adsorbent dose on the adsorption of antibiotics was studied by varying the amount of biochar from 10 to 80 mg, at 30 °C in a 20 mL solution spiked with 2 ppm of the antibiotics. All the classes of antibiotics, that is, β-lactams, fluoroquinolones, and tetracyclines except amoxicillin reached their maximum adsorption rate at a dose of 20 mg of AGB. The adsorption efficiency of amoxicillin increased with the increasing amount of the biochar reaching the maximum adsorption at 80 mg dose of AGB (Figure 3D). Adsorption experiments performed at different temperatures, that is, 30, 40, and 50 °C resulted in the variable adsorption efficiency of the selected antibiotics. Except for amoxicillin, all the other antibiotics exhibited their maximum adsorption efficiency at 30 °C, while at 40 °C, an improved adsorption behavior of amoxicillin was observed with approximately 10 per cent efficiency loss of doxycycline. Moreover, the adsorption capacity of amoxicillin and doxycycline along with chlortetracycline detected a further decline at 50

https://doi.org/10.1021/acsomega.2c07905
ACS Omega 2023, 8, 11065−11075

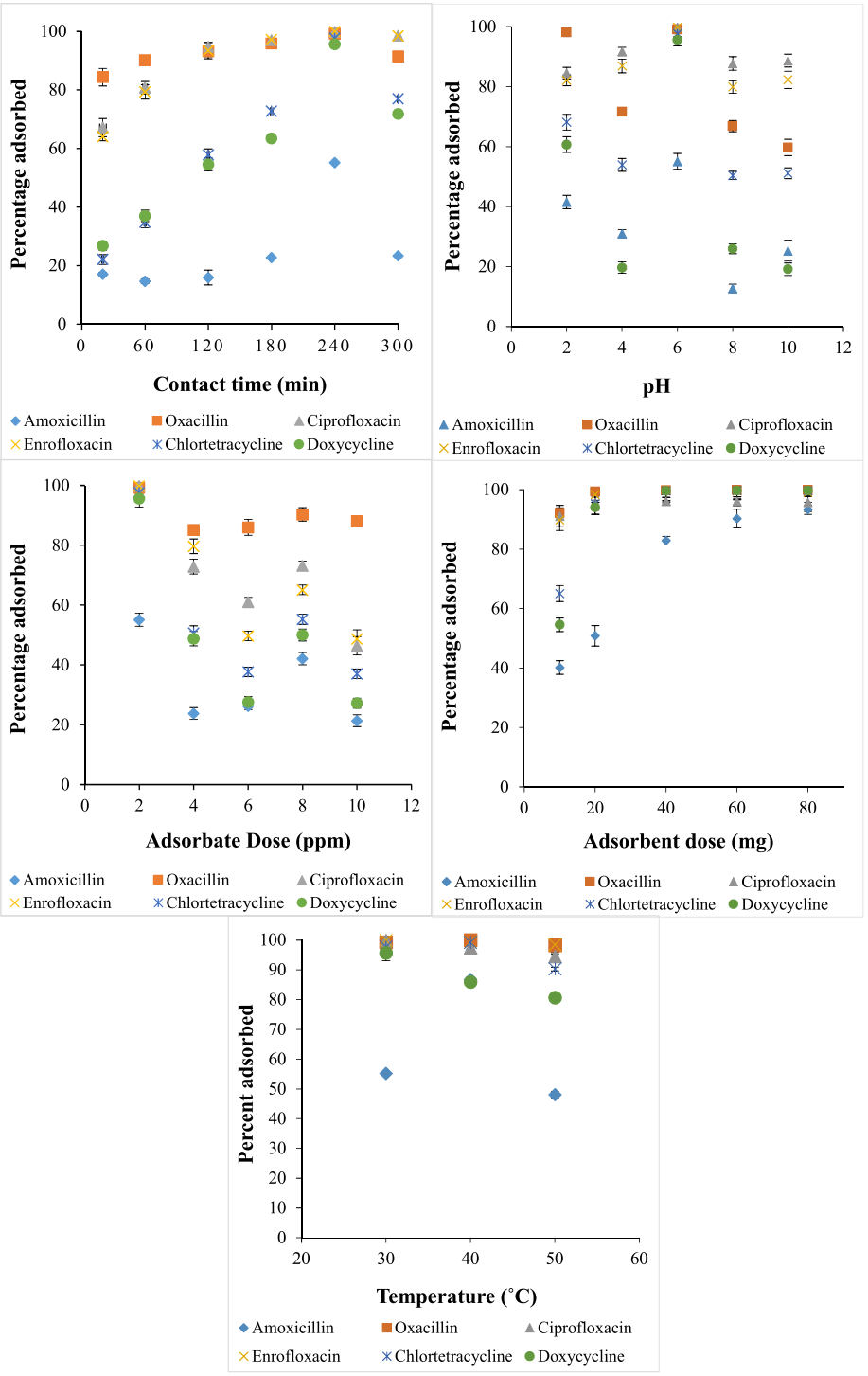

Figure 3. Plot of the parameters affecting the removal efficiency of various antibiotics on to AGB; (A) effect of contact time, (B) pH, (C) adsorbate dose, (D) adsorbent dose, and (E) temperature.

°C (Figure 3E). In conclusion, an overall positive adsorption behavior for all the selected antibiotics at 30 °C which being an environmentally favorable condition is considered the suitable experimental temperature.

3.3. Adsorption Isotherms. *3.3.1. Langmuir Model.* The Langmuir model is the most commonly used model to discuss the adsorption of non-interacting molecules. The model is based on the monolayer adsorption of non-interacting molecules on the homogenous surface. The model is represented by eq 1.

$$\frac{C_e}{q_e} = \frac{C_e}{q_m} + \frac{1}{q_m k_L} \quad (1)$$

where C_e is the adsorbate concentration at equilibrium (mg/L), q_m is the maximum monolayer load capacity (mg/g), q_e is the capacity of adsorption at equilibrium (mg/g), and K_L is the constant in Langmuir isotherm.

3.3.2. Freundlich Model. The Freundlich isotherm is widely used to represent a multilayer adsorption phenomenon on a heterogeneous surface and is represented by eq 2.

https://doi.org/10.1021/acsomega.2c07905
ACS Omega 2023, 8, 11065−11075

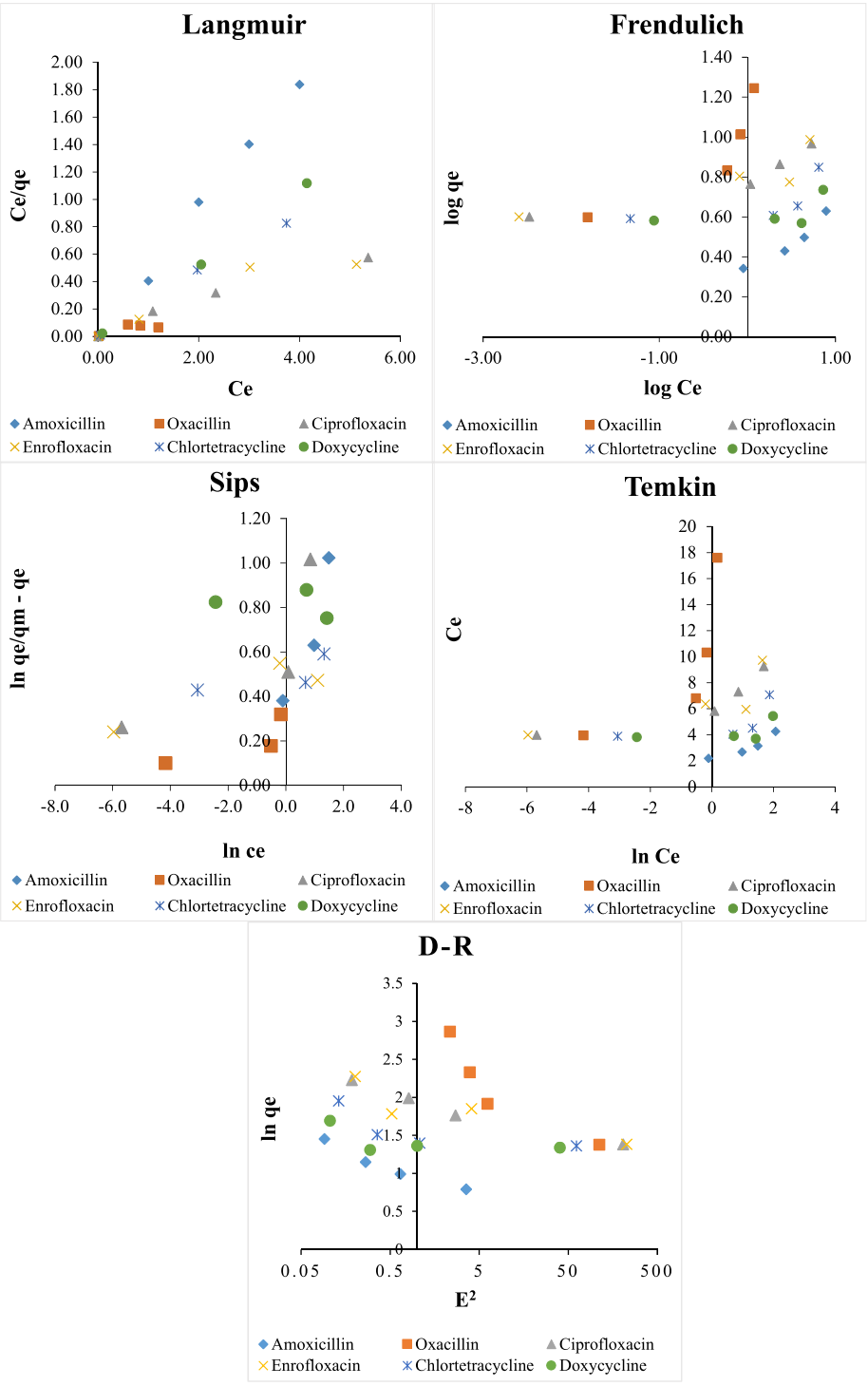

Figure 4. Langmuir, Freundlich, Sips, and Temkin isotherms of the adsorption of antibiotics on AGB.

$$\log q_e = \log k_F + \frac{1}{n}\log c_e \quad (2)$$

where q_e represents the adsorption capacity (mg/g), C_e is the concentration of the adsorbate at equilibrium (mg/L), n is the coefficient of exponent, and k_F is the constant in the Freundlich isotherm.

3.3.3. Sips Model. The Sips model can be defined for homogeneous and heterogeneous systems. It combines the parameters of Freundlich and Langmuir isotherms and can be represented by eq 3.

$$\ln\left[\left(\frac{q_e}{q_m - q_e}\right)\right] = \frac{1}{n}\ln c_e + \ln k_s \quad (3)$$

where k_s is the constant for Sips isotherms.

3.3.4. Temkin Model. This model is based on a multi-layer adsorption process and signifies the decrease of heat of adsorption linearly with increasing coverage.

$$q_e = \left[\frac{RT}{b}\right]\ln A + \left[\frac{RT}{b}\right]\ln c_e \quad (4)$$

https://doi.org/10.1021/acsomega.2c07905
ACS Omega 2023, 8, 11065−11075

where T is the temperature in Kelvin, R is the gas constant (8.314 mol/K), A is Temkin equilibrium binding constant, and b is the constant related to heat of sorption (J mol^{-1}).

3.3.5. Dubinin–Radushkevich (D–R) Adsorption Isotherm. It accounts for the effects of porous structure of adsorbents and expressed as

$$\ln q_e = \ln q_m - K\varepsilon^2 \quad (5)$$

where K is the adsorption constant and ε is Polanyi potential and is calculated by following equation

$$\varepsilon = RT \ln\left[1 + \frac{1}{C}\right] \quad (6)$$

the mean free energy of adsorption E (kJ/mol) is calculated by following equation

$$E = 1/\sqrt{2K} \quad (7)$$

The experiments for isotherm modeling were carried out with the initial concentration ranging from 2 to 10 ppm, time of contact being 240 min, and temperature 30 °C. Based on the correlation coefficient (R^2) and data fits, shown in Figure 4 and Table 1, the adsorption of all the antibiotics fitted well in the Langmuir isotherm model with an exception of oxacillin which was slightly better fitted to Freundlich based on its R^2 value; however, the maximum adsorption capacity (q_m) of oxacillin followed the Langmuir model. The q_m data, in the Langmuir model, for amoxicillin, oxacillin, ciprofloxacin, enrofloxacin, chlortetracycline, and doxycycline were found to be 5.05, 17.42, 9.66, 9.24, 7.15, and 5.40 mg/g, respectively. Furthermore, the value of dimensionless separation factor R_L was found to be <1 for all the tested antibiotics suggesting a favorable adsorption phenomenon. In the D–R isotherm model, the enhanced magnitude of E (>108 kJ/mol) for chlortetracycline, ciprofloxacin, enrofloxacin, and doxycycline, supported the earlier findings and confirmed the adsorption process to be governed by chemical interactions, whereas the adsorption energy for the β-lactam antibiotics was found less than 8 kJ/mol suggesting a physical adsorption mechanism for amoxicillin and oxacillin antibiotics.[30] The differential fitting of the antibiotics in the applied models highlights the dependency of the adsorption mechanism on both the adsorbate and adsorbent characteristics. Analysis of parameters obtained for the Temkin and Sips models showed the selective behavior toward the tested antibiotics reinforcing the importance of structural characteristics of the antibiotics in their adsorption on the AGB (Table 1).

Table 1. Parameters of Langmuir, Freundlich, Temkin, and Sips Isotherm Models for the Adsorption of Antibiotics on AGB

	Langmuir			
	R_L	q_m	k_L	R^2
amoxicillin	0.4786	5.005	0.545	0.9468
oxacillin	0.0180	17.422	27.333	0.5532
ciprofloxacin	0.1740	9.662	2.374	0.9754
enrofloxacin	0.1806	9.242	2.268	0.8805
chlortetracycline	0.3219	7.158	1.053	0.8674
doxycycline	0.2486	5.402	1.511	0.9206
	Freundlich			
	$1/n$	N	k_F	R^2
amoxicillin	0.2922	3.422	0.715	0.9313
oxacillin	0.2713	3.686	0.346	0.7522
ciprofloxacin	0.1003	9.970	0.435	0.8753
enrofloxacin	0.0905	11.050	0.438	0.7512
chlortetracycline	0.0789	12.674	0.512	0.4110
doxycycline	0.0453	22.075	0.542	0.2460
	Temkin			
	$(RT/b) \ln A$	$\ln A$	$RT/b = B$	R^2
amoxicillin	2.095	2.341	0.895	0.8718
oxacillin	2.3143	0.208	11.1312	0.8818
ciprofloxacin	7.0628	11.920	0.5925	0.7821
enrofloxacin	6.9832	12.946	0.5394	0.6237
chlortetracycline	3.3768	6.814	0.4956	0.8344
doxycycline	4.1335	19.730	0.2095	0.2524
	Sips			
	$1/n$	n	k_s	R^2
amoxicillin	0.3754	2.664	1.468	0.8933
oxacillin	0.0410	24.390	1.305	0.6651
ciprofloxacin	0.0882	11.338	2.089	0.6719
enrofloxacin	0.0390	25.641	1.628	0.8366
chlortetracycline	0.0273	36.630	1.657	0.5784
doxycycline	0.0077	129.870	2.267	0.0614
	D–R			
	K	E (kJ/mol)		R^2
amoxicillin	0.139	1.8966		0.660
oxacillin	0.009	7.4535		0.649
ciprofloxacin	0.003	12.9099		0.729
enrofloxacin	0.002	15.8113		0.652
chlortetracycline	0.004	11.1803		0.234
doxycycline	0.003	12.9099		0.108

3.4. Reaction Kinetic Study. *3.4.1. Pseudo-First Order.* The rate of reaction in pseudo-first order kinetics is primarily dependent on one reactant, assuming the concentration of the other reactant is much higher. The linear equation of the reaction is

$$\ln(q_e - q_t) = \ln q_e - k_1 t \quad (8)$$

where q_e = capacity of adsorption at equilibrium (mg/g), q_t = capacity of adsorption at time t (mg/g), and k_1 = rate constant for the first order kinetic reaction.

3.4.2. Pseudo-Second Order. The pseudo-second order reaction is based on the assumption that the rate-limiting step involves chemical adsorption or chemisorption. The equation followed for PSO kinetics is

$$\frac{t}{q_t} = \frac{1}{k_2 q_e^2} + \frac{t}{q_e} \quad (9)$$

where t = time (min), q_t = capacity of adsorption at time t (mg/g), q_e = capacity of adsorption at equilibrium (mg/g), and k_2 = rate constant for the second order kinetic reaction.

3.4.3. Elovich Kinetic Model. This model is based on multilayer adsorption and is represented by eq 7.

$$q_t = \frac{1}{\beta}\ln(\alpha\beta) + \frac{1}{\beta}\ln t \quad (10)$$

where q_t = capacity of adsorption at time t (mg/g), t = time (min), α = adsorption rate constant (mg/g min^{-1}), and β = desorption rate constant (mg/g min^{-1}).

3.4.4. Intraparticle Diffusion Model. Using this method, the rate determining step in aqueous medium is determined. It is expressed as

$$q_t = K_{id} t^{0.5} + C \quad (11)$$

https://doi.org/10.1021/acsomega.2c07905
ACS Omega 2023, 8, 11065−11075

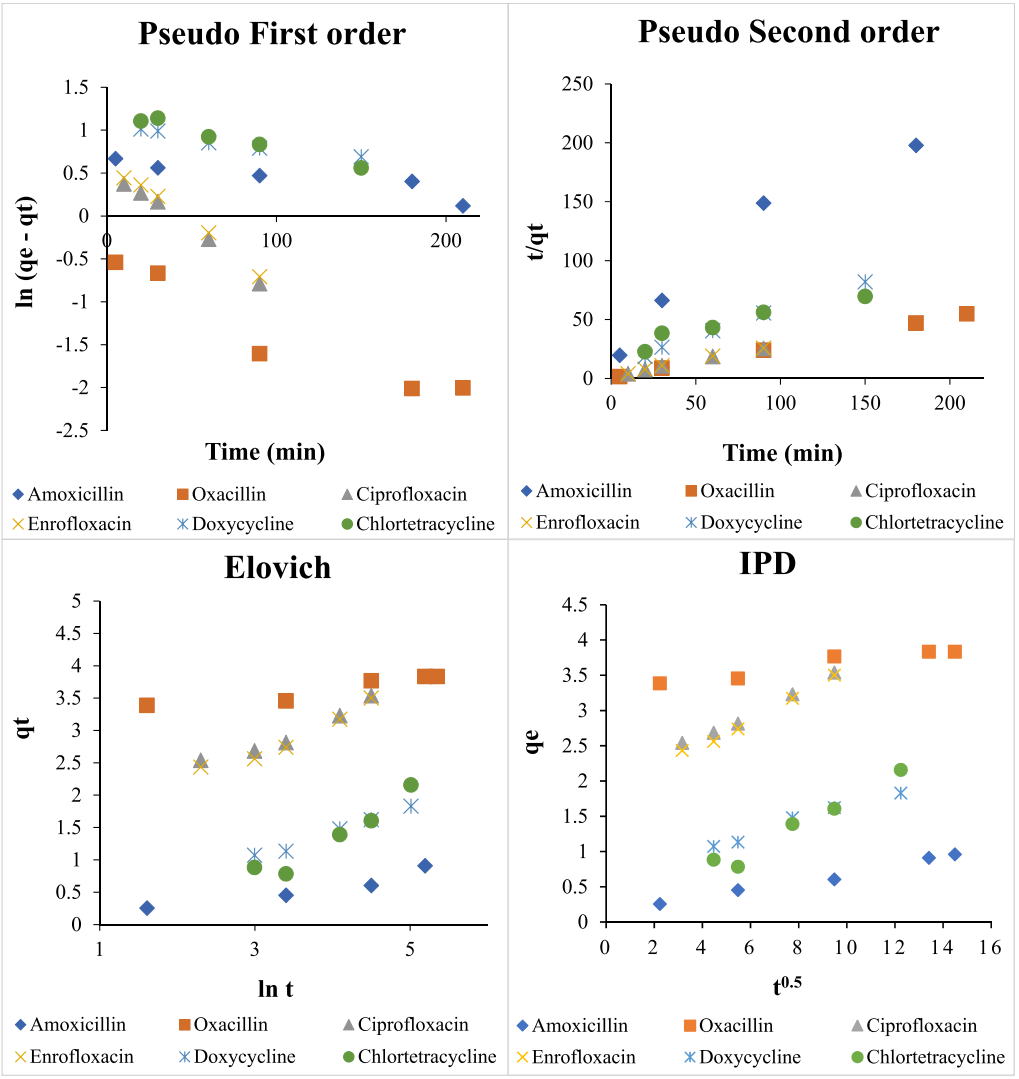

Figure 5. Pseudo-first order, pseudo-second order, Elovich, and IPD kinetic models of the adsorption data of antibiotics on the AGB surface.

where q_t is the measured and model-predicted quantity of antibiotics adsorbed at time t, K_{id} is the intraparticle diffusion rate constant (mg/(gmin$^{0.5}$)), C is the intercept that is evaluated from graph plotted between qt and $t^{0.5}$, and $t^{0.5}$ is the adsorption half-life.[31]

Kinetic studies were conducted between 10 and 210 min at 30 °C. The values for the kinetic constant k_2 of PSO were in good agreement between $q_{e,exp}$ and $q_{e,cal}$, and high correlation coefficient R^2 for all tested antibiotics demonstrated the best fitting by pseudo-second order suggesting chemisorption mechanism of adsorptive removal aligning with the findings of the isotherm studies. The PSO model showed the order of $q_{e,cal}$ values for individual antibiotics as follows: oxacillin > ciprofloxacin > enrofloxacin > chlortetracycline > doxycycline > amoxicillin. The linear part of the IPD indicated the diffusion of antibiotics on AGB, consecutively; lower values of C in the case of chlortetracycline indicated a lower boundary effect, therein, inferring the dominance of IPD only in the adsorption of chlortetracycline on AGB. In rest of the antibiotics, higher values of C indicated that only IPD was not the driving force for adsorption (Figure 5, Table 2).

3.5. Thermodynamic Study. The equations used for the thermodynamic study were as follows

$$\Delta G = -RT \ln k_a \tag{12}$$

and

$$\Delta G = \Delta H - T\Delta S \tag{13}$$

so

$$\ln k_a = \frac{-\Delta H}{RT} + \frac{\Delta S}{R} \tag{14}$$

$$K_a = \frac{C_a}{C_s} \tag{15}$$

where R is the gas constant (J/mol K); T is the temperature in Kelvin; k_a is equilibrium constant; C_a is the concentration of the adsorbate on the adsorbent; C_s is the concentration of the adsorbate in the solution; ΔG = Gibbs free energy (kJ/mol); ΔH = change in Enthalpy (kJ/mol); and ΔS = change in entropy (kJ/mol).

The thermodynamic study was conducted at 30, 40, and 50 °C. The negative values of ΔH and ΔS for all the tested antibiotics suggest an exothermic process of adsorption. In addition, the negative value of ΔG confirmed the spontaneity of the reaction between the adsorbate and adsorbent, while a

https://doi.org/10.1021/acsomega.2c07905
ACS Omega 2023, 8, 11065−11075

Table 2. Parameters of Adsorption Kinetic Models of Antibiotics

	Pseudo-first order			
	q_e,cal (mg gm^{-1})	q_e,exp (mg gm^{-1})	k_1 (min^{-1})	R^2
amoxicillin	1.7081	2.20	0.002481	0.8477
oxacillin	0.6037	3.96	0.000032	0.9145
ciprofloxacin	1.6413	3.99	0.000007	0.9927
enrofloxacin	1.7393	3.99	0.000046	0.9937
chlortetracycline	3.3649	3.90	0.000098	0.9798
doxycycline	2.8451	3.82	0.000186	0.9479
	Pseudo-second order			
	$q_{e,cal}$ (mg gm^{-1})	q_e,exp (mg gm^{-1})	k_2 (g mg^{-1} min^{-1})	R^2
amoxicillin	1.2070	2.20	0.03718	0.9030
oxacillin	3.8730	3.96	26.9104	0.9999
ciprofloxacin	3.7636	3.99	6.91313	0.9946
enrofloxacin	3.7566	3.99	6.09636	0.9937
chlortetracycline	3.6969	3.90	0.46486	0.9792
doxycycline	2.0868	3.82	0.39363	0.9968
	Elovich model			
	$1/\beta$	α	B	R^2
amoxicillin	0.1677	2.4×10^{-1}	5.963	0.8989
oxacillin	0.1330	2.1×109	7.519	0.8967
ciprofloxacin	0.4586	9.2×10^{0}	2.181	0.9395
enrofloxacin	0.4949	5.3×10^{0}	2.021	0.9393
chlortetracycline	0.6634	9.5×10^{-2}	1.507	0.9260
doxycycline	0.3931	2.7×10^{-1}	2.544	0.9873
	IPD model			
	K	C	R^2	
amoxicillin	0.057	0.119	0.987	
oxacillin	0.04	3.293	0.926	
ciprofloxacin	0.161	1.981	0.991	
enrofloxacin	0.174	1.823	0.990	
chlortetracycline	0.176	−0.025	0.964	
doxycycline	0.101	0.625	0.976	

higher temperature was not suited for the spontaneous adsorption of amoxicillin on AGB (Table 3).

4. CONCLUSIONS

The present work was conducted considering the rising global concerns about the pandemic of antibiotic resistance. A novel application of ginger waste biochar was established for the removal of six antibiotics belonging to three different classes. The activation of the prepared biochar with zinc chloride resulted in improved surface area and porosity, hence facilitating the efficient remediation of selected antibiotics from water. The characteristics of AGB were studied by FTIR, SEM-EDAX, TGA, and BET experiments. The mechanistic adsorption of commonly used antibiotics from diverse classes on AGB was thoroughly studied. Results of the batch experiments revealed that the Langmuir model was the best fit for isothermal data highlighting the monolayer adsorption on a homogeneous AGB surface of all six antibiotics. Best fit values of kinetic data in pseudo-second order kinetics confirmed the chemisorption mechanism of adsorption to adsorbents on the adsorbate surface and could be mediated by the electrostatic interactions between the positively charged metal ions of adsorbate and negatively charged/electron−rich interaction sites of the adsorbent. Evaluation of the thermodynamic parameters suggested

Table 3. Thermodynamic Parameters of Antibiotic Adsorption on the AGB

antibiotics	temperature (Kelvin)	ΔH (kJ/mol)	ΔS (kJ/mol K)	ΔG (kJ/mol)
amoxicillin	303.15	−9.94	−0.03	−0.52
	313.15			−4.88
	323.15			0.21
oxacillin	303.15	−34.44	−0.07	−12.23
	313.15			−12.62
	323.15			−10.74
ciprofloxacin	303.15	−145.41	−0.43	−16.09
	313.15			−9.46
	323.15			−7.61
enrofloxacin	303.15	−102.45	−0.28	−16.79
	313.15			−12.70
	323.15			−11.16
chlortetracycline	303.15	−76.27	−0.21	−10.93
	313.15			−11.39
	323.15			−6.56
doxycycline	303.15	−67.87	−0.20	−7.76
	313.15			−4.70
	323.15			−3.82

favorable adsorption of antibiotics on the AGB surface. The negative values of Gibb's free energy (ΔG) indicated a spontaneous reaction between the adsorbent and the adsorbate. The performed study showed high adsorption capacities to effectively remove all the tested antibiotics from the aqueous medium with a removal efficiency of more than 95 per cent for all the tested antibiotics except amoxicillin (86 per cent). To summarize, AGB being a waste-derived ecofriendly and economical adsorbent material has emerged as a potential adsorbate for the removal of emerging and health-challenging contaminants such as antibiotics from aqueous solution with promising adsorption efficiency.

■ ASSOCIATED CONTENT

Supporting Information

The Supporting Information is available free of charge at https://pubs.acs.org/doi/10.1021/acsomega.2c07905.

Representative extracted ion chromatograms (XICs) and mass spectra of the antibiotics (PDF)

■ AUTHOR INFORMATION

Corresponding Author

Akhilesh K. Yadav − *Analytical Chemistry Laboratory, Regulatory Toxicology Group, CSIR-Indian Institute of Toxicology Research, (CSIR-IITR), Lucknow 226001 Uttar Pradesh, India; Academy of Scientific and Innovative Research (AcSIR), Ghaziabad 201002, India;* orcid.org/0000-0003-0269-3050; Email: akhilesh.yadav1@iitr.res.in, akhil.aky@gmail.com

Authors

Roshni Meghani − *Food Toxicology Laboratory, Food Drug and Chemical Toxicology Group, CSIR-Indian Institute of Toxicology Research, (CSIR-IITR), Lucknow 226001 Uttar Pradesh, India*

Vaibhavi Lahane − *Analytical Chemistry Laboratory, Regulatory Toxicology Group, CSIR-Indian Institute of Toxicology Research, (CSIR-IITR), Lucknow 226001 Uttar*

https://doi.org/10.1021/acsomega.2c07905
ACS Omega 2023, 8, 11065−11075

Pradesh, India; Academy of Scientific and Innovative Research (AcSIR), Ghaziabad 201002, India

Sumana Y. Kotian − *Analytical Chemistry Laboratory, Regulatory Toxicology Group, CSIR-Indian Institute of Toxicology Research, (CSIR-IITR), Lucknow 226001 Uttar Pradesh, India*

Sneh Lata − *Analytical Chemistry Laboratory, Regulatory Toxicology Group, CSIR-Indian Institute of Toxicology Research, (CSIR-IITR), Lucknow 226001 Uttar Pradesh, India; Academy of Scientific and Innovative Research (AcSIR), Ghaziabad 201002, India*

Swati Tripathi − *Analytical Chemistry Laboratory, Regulatory Toxicology Group, CSIR-Indian Institute of Toxicology Research, (CSIR-IITR), Lucknow 226001 Uttar Pradesh, India*

Kausar M. Ansari − *Food Toxicology Laboratory, Food Drug and Chemical Toxicology Group, CSIR-Indian Institute of Toxicology Research, (CSIR-IITR), Lucknow 226001 Uttar Pradesh, India; Academy of Scientific and Innovative Research (AcSIR), Ghaziabad 201002, India;* orcid.org/0000-0001-7879-2771

Complete contact information is available at: https://pubs.acs.org/10.1021/acsomega.2c07905

Author Contributions

R.M. and V.L. contributed equally. Conceptualization and plan execution, A.K.Y.; experimentation, methodology and data interpretation: R.M. and V.L.; statistical analysis and manuscript writing: R.M., S.Y.K., S.L., and S.T.; proofreading and manuscript drafting: A.K.Y. and K.M.A.

Notes

The authors declare no competing financial interest.

■ ACKNOWLEDGMENTS

The authors are thankful to the Director, CSIR-Indian Institute of Toxicology Research, Lucknow, India, for financial support. Support from Central Instrument facility, CSIR-CIMAP, is highly acknowledged for facilitating the SEM-EDAX analysis. We would also like to thank Dr Satyakam Patnaik for providing instrumental facilities of the BET surface area analyzer, TGA, and ATR-FTIR.

■ REFERENCES

(1) World Health Organization. *Antimicrobial Resistance-Global Report on Surveillance*; World Health Organization, 2014.

(2) Solomon, S. L.; Oliver, K. B. Antibiotic resistance threats in the United States: Stepping back from the brink. *Am. Fam. Physician* **2014**, *89*, 938−941.

(3) O'Neill, J. *Antimicrobial Resistance: Tackling a Crisis for the Health and Wealth of Nations*. Review on Antimicrobial Resistance Chaired by Jim O'Neill, 2014.

(4) Kotwani, A.; Joshi, J.; Kaloni, D. Pharmaceutical effluent: a critical link in the interconnected ecosystem promoting antimicrobial resistance. *Environ. Sci. Pollut. Res.* **2021**, *28*, 32111−32124.

(5) Samal, K.; Mahapatra, S.; Hibzur Ali, M. Pharmaceutical wastewater as Emerging Contaminants (EC): Treatment technologies, impact on environment and human health. *Energy Nexus* **2022**, *6*, 100076.

(6) Landers, T. F.; Cohen, B.; Wittum, T. E.; Larson, E. L. A review of antibiotic use in food animals: Perspective, policy, and potential. *Public Health Rep.* **2012**, *127*, 4−22.

(7) Van Boeckel, T. P.; Brower, C.; Gilbert, M.; Grenfell, B. T.; Levin, S. A.; Robinson, T. P.; Teillant, A.; Laxminarayan, R. Global trends in antimicrobial use in food animals. *Proc. Natl. Acad. Sci.* **2015**, *112*, 5649−5654.

(8) Sachi, S.; Ferdous, J.; Sikder, M. H.; Hussani, S. M. Antibiotic residues in milk: Past, present, and future. *J. Adv. Vet. Anim. Res.* **2019**, *6*, 315−332.

(9) Li, N.; Ho, K. W. K.; Ying, G. G.; Deng, W. J. Veterinary antibiotics in food, drinking water, and the urine of preschool children in Hong Kong. *Environ. Int.* **2017**, *108*, 246−252.

(10) Wang, Y.; Zhao, X.; Zang, J.; Li, Y.; Dong, X.; Jiang, F.; Wang, N.; Jiang, L.; Jiang, Q.; Fu, C. Estimates of Dietary Exposure to Antibiotics among a Community Population in East China. *Antibiotics* **2022**, *11*, 407.

(11) Fair, R. J.; Tor, Y. Antibiotics and bacterial resistance in the 21st century. *Perspect. Med. Chem.* **2014**, *6*, 25−64.

(12) Alameri, A. A.; Alfilh, R. H.; Awad, S. A.; Zaman, G. S.; Al-Musawi, T. J.; Joybari, M. M.; Balarak, D.; McKay, G. Ciprofloxacin adsorption using magnetic and ZnO nanoparticles supported activated carbon derived from Azolla filiculoides biomass. *Biomass Convers. Biorefin.* **2022**, 1−14.

(13) Balarak, D.; Mahvi, A. H.; Shim, M. J.; Lee, S. M. Adsorption of ciprofloxacin from aqueous solution onto synthesized NiO: isotherm, kinetic and thermodynamic studies. *Desalin. Water Treat.* **2021**, *212*, 390−400.

(14) Andreozzi, R.; Canterino, M.; Marotta, R.; Paxeus, N. Antibiotic removal from wastewaters: the ozonation of amoxicillin. *J. Hazard Mater.* **2005**, *122*, 243−250.

(15) Ahmed, M. B.; Zhou, J. L.; Ngo, H. H.; Guo, W.; Johir, M. A. H.; Sornalingam, K. Single and competitive sorption properties and mechanism of functionalized biochar for removing sulfonamide antibiotics from water. *Chem. Eng. J.* **2017**, *311*, 348−358.

(16) Li, C.; Zhu, X.; He, H.; Fang, Y.; Dong, H.; Lü, J.; Li, J.; Li, Y. Adsorption of two antibiotics on biochar prepared in air-containing atmosphere: Influence of biochar porosity and molecular size of antibiotics. *J. Mol. Liq.* **2019**, *274*, 353−361.

(17) Balarak, D.; Mahvi, A. H.; Shahbaksh, S.; Wahab, M. A.; Abdala, A. Adsorptive removal of azithromycin antibiotic from aqueous solution by azolla filiculoides-based activated porous carbon. *Nanomaterials* **2021**, *11*, 3281.

(18) Yilmaz, M.; Al-Musawi, T. J.; Saloot, M. K.; Khatibi, A. D.; Baniasadi, M.; Balarak, D. Synthesis of activated carbon from Lemna minor plant and magnetized with iron (III) oxide magnetic nanoparticles and its application in removal of ciprofloxacin. *Biomass Convers. Biorefin.* **2022**, 1−14.

(19) Nartey, O. D.; Zhao, B. Biochar preparation, characterization, and adsorptive capacity and its effect on bioavailability of contaminants: An overview. *Adv. Mater. Sci. Eng.* **2014**, *2014*, 715398.

(20) Guizani, C.; Jeguirim, M.; Valin, S.; Limousy, L.; Salvador, S. Biomass chars: The effects of pyrolysis conditions on their morphology, structure, chemical properties and reactivity. *Energies* **2017**, *10*, 796.

(21) Fahmi, A. H.; Samsuri, A. W.; Jol, H.; Singh, D. Physical modification of biochar to expose the inner pores and their functional groups to enhance lead adsorption. *RSC Adv.* **2018**, *8*, 38270−38280.

(22) Alnajrani, M. N.; Alsager, O. A. Removal of antibiotics from water by polymer of intrinsic microporosity: Isotherms, kinetics, thermodynamics, and adsorption mechanism. *Sci. Rep.* **2020**, *10*, 794.

(23) Mei, Y.; Xu, J.; Zhang, Y.; Li, B.; Fan, S.; Xu, H. Effect of Fe-N modification on the properties of biochars and their adsorption behavior on tetracycline removal from aqueous solution. *Bioresour. Technol.* **2021**, *325*, 124732.

(24) Liou, T. H. Development of mesoporous structure and high adsorption capacity of biomass-based activated carbon by phosphoric acid and zinc chloride activation. *Chem. Eng. J.* **2010**, *158*, 129−142.

(25) Omran, M.; Fabritius, T.; Heikkinen, E. P.; Chen, G. Dielectric properties and carbothermic reduction of zinc oxide and zinc ferrite by microwave heating. *R. Soc. Open Sci.* **2017**, *4*, 170710.

(26) Zhao, F.; Shan, R.; Li, W.; Zhang, Y.; Yuan, H.; Chen, Y. Synthesis, Characterization, and Dye Removal of ZnCl2-Modified Biochar Derived from Pulp and Paper Sludge. *ACS Omega* **2021**, *6*, 34712−34723.

(27) Fu, S.; Fang, Q.; Li, A.; Li, Z.; Han, J.; Dang, X.; Han, W. Accurate characterization of full pore size distribution of tight sandstones by low-temperature nitrogen gas adsorption and high-pressure mercury intrusion combination method. *Energy Sci. Eng.* **2021**, *9*, 80−100.
(28) Peng, B.; Chen, L.; Que, C.; Yang, K.; Deng, F.; Deng, X.; Shi, G.; Xu, G.; Wu, M. Adsorption of antibiotics on graphene and biochar in aqueous solutions induced by π-π interactions. *Sci. Rep.* **2016**, *6*, 31920.
(29) Wang, H.; Lou, X.; Hu, Q.; Sun, T. Adsorption of antibiotics from water by using Chinese herbal medicine residues derived biochar: Preparation and properties studies. *J. Mol. Liq.* **2021**, *325*, 114967.
(30) Hu, Q.; Zhang, Z. Application of Dubinin-Radushkevich isotherm model at the solid/solution interface: A theoretical analysis. *J. Mol. Liq.* **2019**, *277*, 646−648.
(31) Kumar, A.; Prasad, S.; Saxena, P. N.; Ansari, N. G.; Patel, D. K. Synthesis of an Alginate-Based Fe3O4-MnO2 Xerogel and Its Application for the Concurrent Elimination of Cr(VI) and Cd(II) from Aqueous Solution. *ACS Omega* **2021**, *6*, 3931−3945.

https://doi.org/10.1021/acsomega.2c07905
ACS Omega 2023, 8, 11065−11075